⌘ *Author's Choice*

THE JOURNAL OF BIOLOGICAL CHEMISTRY VOL. 286, NO. 25, pp. 22113–22121, June 24, 2011

Anchored Protein Kinase A Recruitment of Active Rac GTPase[S]

Received for publication, February 17, 2011, and in revised form, March 28, 2011 Published, JBC Papers in Press, April 1, 2011, DOI 10.1074/jbc.M111.232660

Jeremy S. Logue[‡§], Jennifer L. Whiting[‡¶], Brian Tunquist[‡1], Lorene K. Langeberg[‡¶], and John D. Scott[‡¶2]

From the [‡]Howard Hughes Medical Institute, [¶]Department of Pharmacology, and the [§]Molecular and Cellular Biology Program, University of Washington School of Medicine, Seattle, Washington 98195

Protein kinase A-anchoring proteins (AKAPs) influence fundamental cellular processes by directing the cAMP-dependent protein kinase (PKA) toward its intended substrates. In this report we describe the identification and characterization of a ternary complex of AKAP220, the PKA holoenzyme, and the IQ domain GTPase-activating protein 2 isoform (IQGAP2) that is enriched at cortical regions of the cell. Formation of an IQGAP2-AKAP220 core complex initiates a subsequent phase of protein recruitment that includes the small GTPase Rac. Biochemical and molecular biology approaches reveal that PKA phosphorylation of Thr-716 on IQGAP2 enhances association with the active form of the Rac GTPase. Cell-based experiments indicate that overexpression of an IQGAP2 phosphomimetic mutant (IQGAP2 T716D) enhances the formation of actin-rich membrane ruffles at the periphery of HEK 293 cells. In contrast, expression of a nonphosphorylatable IQGAP2 T716A mutant or gene silencing of AKAP220 suppresses formation of membrane ruffles. These findings imply that IQGAP2 and AKAP220 act synergistically to sustain PKA-mediated recruitment of effectors such as Rac GTPases that impact the actin cytoskeleton.

Spatial control of enzymes helps to focus and synchronize the flow of information through signal transduction pathways. Often this occurs through the assembly of multiprotein complexes where enzymes are precisely arranged to receive activation signals and located in proximity to substrates (1). These complexes are frequently maintained by protein-protein interactions that proceed through scaffolding or anchoring proteins or specialized enzyme-targeting subunits (2). Prime examples of such signal transduction-enhancing factors include protein phosphatase 1-targeting subunits and protein kinase A-anchoring proteins (AKAPs)[3] (3, 4). AKAPs compartmentalize the cAMP-dependent protein kinase (PKA) through binding of the regulatory (RI or RII) subunit dimer (5, 6). The first anchoring proteins were detected as protein contaminants that co-purified with RII subunits on cAMP-agarose affinity columns (7). Later, far Western blotting protocols that utilized RII as the probe, expression cloning strategies and yeast two-hybrid analyses discovered many more members of the AKAP family (8, 9). Currently, there are 46 genes in this burgeoning group that are classified on the basis of their ability to interact with PKA (4). However, many AKAPs target other cAMP-responsive enzymes such as adenylyl cyclases, Epac guanine nucleotide exchange factors, and phosphodiesterases (10–15). By positioning cAMP effector proteins of differing action near their substrates, AKAPs broaden the scope of this essential second messenger. Perhaps not surprisingly, AKAPs also target other classes of signal transduction and signal termination enzymes. For example, the product of the AKAP11 gene is a 220-kDa anchoring protein called AKAP220 (16). We have previously shown that this anchoring protein sequesters PKA and protein phosphatase 1 at peroxisomes (17, 18). Subsequent studies have shown that AKAP220 complexes also contain glycogen synthase kinase-3 (17, 18). Yet, the full repertoire of AKAP220-binding partners is unknown.

In this report, we define a signaling network that includes AKAP220, PKA, and the cytoskeletal scaffolding protein IQ domain GTPase-activating protein 2 (IQGAP2). IQGAPs are multipurpose scaffolding proteins that bind a number of effector proteins, including the small GTPases Rac and Cdc42, and microtubule plus end-binding proteins. IQGAPs orchestrate these signals to regulate dynamic changes in actin and microtubules, respectively (19–23). Accordingly, IQGAPs have been implicated in the synchronization of signaling events that underlie cell migration, cell growth and division, and the establishment of cellular asymmetry (19–21, 24, 25). We show that IQGAP2 and AKAP220 form a core complex that favors PKA-dependent recruitment of the small GTPase Rac to augment certain aspects of actin remodeling.

EXPERIMENTAL PROCEDURES

Antibodies—Anti-AKAP220 antibody was affinity-purified from sera produced by immunizing rabbits with a fragment encoding the first 300 amino acids of bacterially expressed and purified mouse AKAP220. Rabbit polyclonal anti-GFP antibody (Invitrogen), mouse monoclonal anti-V5 (Invitrogen), mouse monoclonal anti-HA (Sigma), mouse monoclonal anti-PKA_c (BD Biosciences), mouse monoclonal anti-calmodulin (Millipore), mouse monoclonal anti-Rac (Millipore), rabbit polyclonal anti-phospho-PKA substrates (Cell Signaling Technology), and mouse monoclonal anti-actin (Sigma) were used

[S] The on-line version of this article (available at http://www.jbc.org) contains supplemental Figs. S1–S6.

⌘ *Author's Choice*—Final version full access.

[1] Present address: Array BioPharma, Boulder, CO 80301.

[2] Supported, in whole or in part, by National Institutes of Health Grant DK54441. To whom correspondence should be addressed: University of Washington, 1959 Pacific Ave. N.E., Box 357750, Seattle, WA 98195. Fax: 206-616-3386; E-mail: scottjdw@u.washington.edu.

[3] The abbreviations used are: AKAP, protein kinase A-anchoring protein; C subunit, catalytic subunit; IQGAP, IQ domain GTPase-activating protein; R subunit, regulatory subunit; ri, ruffling index; AKAP, A-kinase anchoring protein; IQGAP, IQ-domain GTPase activating protein.

as stated in the text. Rabbit polyclonal anti-IQGAP2 antibody was kindly provided by Kozo Kaibuchi (Nagoya University).

Cells and Reagents—HEK 293 and COS cells were cultured in DMEM supplemented with 10% FBS and penicillin/streptomycin/Fungizone. Cells were transfected with plasmids using Lipofectamine 2000 (Invitrogen). Plasmids encoding IQGAP2 were constructed using the Gateway cloning system (Invitrogen) according to the manufacturer's protocol. IQGAP2 point mutants were generated using a QuikChange Site-directed Mutagenesis kit (Stratagene) according to the manufacturer's protocol. The preparation of digoxigenin-labeled RIIα has been described previously (8). A23187 and H-89 were purchased from Calbiochem. Stearated Ht-31 and stearated Ht-31 Pro were from Promega.

Cell Treatment and Lysis—Cells were washed in cold buffer containing 150 mM NaCl and 25 mM Tris-HCl, pH 7.4. Lysis took place in 150 mM NaCl, 25 mM Tris-HCl, pH 7.4, 1% Nonidet P-40, 10 mM NaF, 1 mM sodium orthovanadate, 100 nM microcystin (Calbiochem), and protease inhibitor mixture (Pierce). Wash and lysis buffers contained 1 mM $CaCl_2$ or 1 mM EGTA and 1 mM EDTA where indicated. Lysates were cleared by centrifugation at 16,400 rpm for 10 min at 4 °C. Proteins were immunoprecipitated for ~3 h at 4 °C.

Mass Spectrometry—HEK 293 cells were transfected with plasmids expressing FLAG-AKAP220. After lysis, immunocomplexes were isolated using FLAG-M2 agarose (Sigma) and separated by SDS-PAGE on 4–12% NuPAGE gels (Invitrogen). Gels were stained with GelCode Blue (Thermo-Pierce), and bands were excised. Proteins were identified as described (26).

Activity and Immunokinase Assays—In PKA activity assays, catalytic (C) subunit was eluted from immunoprecipitates with 100 μM cAMP (Sigma). A standard filter-based assay was then carried out using Leu-Arg-Arg-Ala-Ser-Leu-Gly (Kemptide) as the substrate (LRRASLG; Calbiochem) (27). Prior to immunokinase assays, purified immunocomplexes were washed twice in kinase buffer (50 mM KCl, 25 mM Tris, 7.4, 10 mM $MgCl_2$, 2 mM $CaCl_2$, 0.1 mg/ml BSA, and 50 μM ATP). Phosphorylation reactions were performed in kinase buffer supplemented with 0.2 μg of PKA catalytic subunits (New England Biolabs) and [γ-^{32}P]ATP for 20 min at room temperature. 10 μM (final) PKI(5–24) (Promega) was included in some reactions to block kinase activity. Reactions were stopped by washing twice with lysis buffer and adding NuPAGE sample buffer (Invitrogen). Reactions were separated by SDS-PAGE on 4–12% NuPAGE gels (Invitrogen), transferred to nitrocellulose, and analyzed by autoradiography.

Immunofluorescence Staining—HEK 293 cells were cultured on glass coverslips (no. 1.5) coated with bovine collagen (Sigma). When staining for AKAP220, IQGAP2, or actin, cells were fixed using cold methanol containing 1% paraformaldehyde for 20 min on ice. Cells stained with fluorescently conjugated phalloidin were fixed using 4% paraformaldehyde in PBS for 20 min at room temperature. Blocking, antibody incubation, and washing steps were done using PBS containing 0.1% Triton X-100, 1% BSA, 1% fish gelatin, and 0.1% sodium azide. Antibodies were incubated for 1 h at room temperature. Alexa Fluor-conjugated secondary antibodies were from Invitrogen. Coverslips were mounted on glass slides using ProLong Gold (Invitrogen). Nuclei were stained using the novel far-red fluorescent DNA dye DRAQ5 (Axxora Platform). Cells were imaged on a Zeiss LSM 510 META confocal microscope using a 63 × Plan-Apochromat oil immersion lens (NA 1.4). Image analyses were performed using ImageJ (National Institutes of Health).

Quantification of Membrane Ruffling—The ruffling index was calculated according to the method of Li *et al.* with minor modifications (28). Images of cells expressing GFP or GFP-IQGAP2 constructs were quantified for the extent of membrane ruffling by comparing images of protein expression with staining for F-actin near the cell membrane in ImageJ. Cells without ruffles were given a score of 0, and cells with maximal ruffling (covering 100% of the cell surface) were given a score of 3, and an average was determined for each population. Statistical significance was determined by an unpaired two-tailed Student's *t* test using GraphPad software.

RESULTS AND DISCUSSION

Identification and Characterization of an AKAP220-PKA-IQGAP2 Ternary Complex—Assembly of macromolecular complexes often requires that anchoring and scaffolding proteins sequester enzymes with substrates and effectors. This notion was borne out in a mass spectrometry-based screen. Recombinant FLAG-tagged AKAP220 was expressed in HEK 293 cells. AKAP220 and associated proteins were enriched by affinity chromatography on anti-FLAG agarose. After extensive washing the protein complex was eluted and separated by SDS-PAGE, and binding partners were identified by tandem mass spectroscopy. The detection of peptides derived from AKAP220 and the regulatory (R) and catalytic (C) subunits of PKA served as internal controls. In addition, 36 peptides corresponding to the IQGAP2 isoform and 2 peptides matching the IQGAP3 isoform were identified (supplemental Fig. S1). We chose to investigate the clustering of IQGAP2 with anchored PKA because it contains consensus substrate sites for this protein kinase (details below under "IQGAP2 Is an Anchored PKA Substrate").

The existence of a cellular IQGAP2-AKAP220-PKA ternary complex was validated in five ways. First, immunoprecipitation of endogenous AKAP220 from HEK 293 cells resulted in the co-fractionation of IQGAP2 and C subunit of PKA as assessed by immunoblotting (Fig. 1*A*, *top* and *middle panels*, *lane 2*). Second, reciprocal studies demonstrated that enrichment for recombinant V5-tagged IQGAP2 favored the co-precipitation of AKAP220 and C subunit (Fig. 1*B*, *top* and *middle panels*, *lane 2*). Third, endogenous IQGAP2 was isolated in complex with AKAP220 from brain extracts and detected by immunoblotting (Fig. 1*C*, *top panel*, *lane 2*). The RII overlay was used as a fourth means to assess whether GFP-tagged IQGAP2 bound to other AKAPs. A single RII binding band of ~220 kDa (Fig. 1*D*, *top panel*, *lane 2*) with the migration pattern that corresponded to AKAP220 (Fig. 1*D*, *middle panel*, *lane 2*) was detected by this approach.

Last, we measured PKA activity associated with IQGAP2 immune complexes (Fig. 1, *E* and *F*). Gene silencing of AKAP220 prevented the co-purification of RII and C subunits of the kinase as assessed by immunoblotting (Fig. 1*E*, *lane 1*).

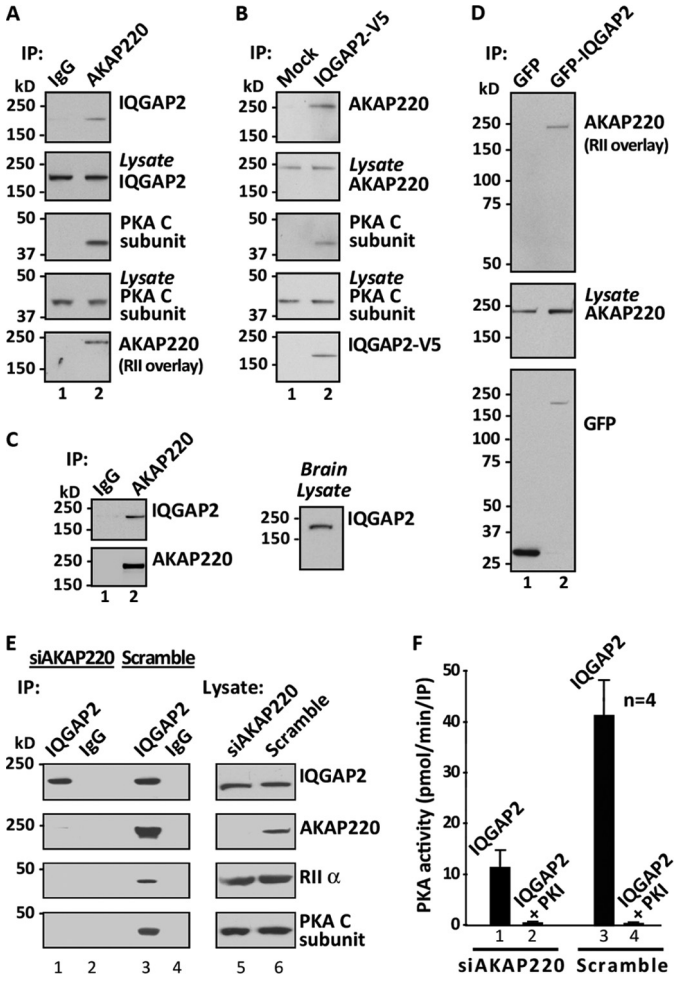

FIGURE 1. **Biochemical validation of the AKAP220-PKA-IQGAP2 ternary complex.** *A*, AKAP220 immune complexes from HEK 293 cell lysates were probed for co-fractionation for V5-tagged IQGAP2 (*top*), C subunit of PKA (*middle*), and AKAP220 (*bottom*). Loading controls for IQGAP2 (*upper middle*) and C subunit of PKA (*lower middle*) are included. *B*, co-purification of AKAP220 (*top*) and C subunit of PKA (*middle*) with V5-tagged IQGAP2 immune complexes (*bottom*) are shown. Loading controls for AKAP220 (*upper middle*) and C subunit of PKA (*lower middle*) are included. *C*, AKAP220 was immunoenriched from mouse brain extracts. Co-purification of endogenous IQGAP2 (*top*) was determined by immunoblotting. Loading controls depict the levels of AKAP220 in immune complexes (*middle*) and IQGAP2 in brain extracts (*bottom*). *D*, GFP-tagged IQGAP2 was immunoprecipitated from COS cells and screened for interaction with AKAPs by RII overlay (*top*). AKAP220 was detected by immunoblotting (*middle*), and levels of immunoprecipitated GFP and GFP-IQGAP2 (*bottom*) are indicated. *E*, gene silencing of AKAP220 reduces the co-purification of PKA subunits with IQGAP2. Incubation with siAKAP220 oligonucleotides for 24 h (*lanes 2*, *5*, and *6*) suppressed expression levels of AKAP220 as assessed by immunoblotting (*center top*; *lane 2*). Loading controls demonstrated that treatment with scrambled siRNAs (*lanes 1*, *3*, and *4*) had no effect on protein levels of IQGAP2 (*top*), AKAP220 (center top), RII (center bottom) or the C subunit of PKA (*bottom*). *F*, PKA activity measurements from IQGAP2 immunoprecipitates using Kemptide as a substrate are presented. Treatment conditions are indicated under each column. All data presented are representative of at least three independent experiments.

Depletion of the anchoring protein resulted in 3.8-fold ($n = 4$) reduction in IQGAP2-associated PKA activity compared with scrambled siRNA controls (Fig. 1*F*, compare *columns 1* and *3*). All PKA activity was blocked in the presence of the PKI(5–24) peptide inhibitor (Fig. 1*F*, *columns 2* and *4*). Immunoblot analysis of cell lysates confirmed that AKAP220 knockdown did not have compensatory effects on protein levels of IQGAP2 or the RII and C subunits of PKA (Fig. 1*E*, *all panels*, *lane 5*). Taken together, the data in Fig. 1 verify that AKAP220 and IQGAP2 are components of a signaling network that includes the type II PKA holoenzyme. These protein-protein interactions provide a foundation for the assembly of a larger protein complex that responds to diffusible intracellular signals.

Aspects of IQGAP function are calcium-dependent. This frequently involves calmodulin binding to the IQ domains that give the scaffolding protein its name (29–32). IQGAP2 interaction with AKAP220 may proceed through a similar mechanism as isolation of an AKAP220-IQGAP2 complex is enhanced in cells treated with the calcium ionophore A23187 (supplemental Fig. S2). Formation of this core complex sets up a framework for the integration of other second messenger signals. We propose that extracellular cues that stimulate cAMP production are received by an AKAP220-PKA-IQGAP2 ternary complex. Although cAMP binding to PKA regulatory subunits does not affect R association with AKAPs (8, 33), this second messenger releases active C subunits from the PKA holoenzyme (34, 35). This creates a microenvironment within the immediate vicinity of AKAP220 and IQGAP2 where PKA phosphorylation is favored. Local zones of amplified PKA activity may be a hallmark of AKAP220 complexes as this anchoring protein is believed to contain multiple binding sites for the type I and type II PKA holoenzymes (36).

IQGAP2 Is an Anchored PKA Substrate—In keeping with a now well established view that AKAPs augment cAMP-responsive events (37) we postulated that AKAP220 constrains PKA to favor phosphorylation of IQGAP2. *In vitro* labeling experiments demonstrated that IQGAP2 was a PKA substrate whereas IQGAP1 was refractory to this kinase (Fig. 2*A*). A computer-aided search identified consensus PKA substrate motifs (RR*X*S/T) at Thr-716 and Thr-881 in IQGAP2 (Fig. 2*B*, *boxes*). Equivalent sites are not present in the IQGAP1 or IQGAP3 isoforms (Fig. 2*B*, *boxes*).

Characterization of these putative phosphorylation sites involved incubation of affinity purified V5-tagged IQGAP2 or mutants with [γ-^{32}P]ATP and purified C subunit of PKA (Fig. 2, *C* and *D*). Wild-type IQGAP2 readily incorporated ^{32}P as assessed by autoradiography (Fig. 2, *C*, *top panel*, *lane 1*, and *D*). This effect was blocked in the presence of PKI(5–24) inhibitor peptide (Fig. 2, *C*, *top panel*, *lane 2*, and *D*). Substitution of Thr-716 with Ala (T716A) reduced ^{32}P incorporation into IQGAP2 (Fig. 2, *C*, *top panel*, *lane 3*, and *D*). In contrast, ^{32}P incorporation into the IQGAP2 T881A mutant was similar to the wild-type protein (Fig. 2, *C*, *top panel*, *lane 4*, and *D*). Additional control experiments showed that ^{32}P incorporation was reduced to base-line levels when an IQGAP T716A/T881A double mutant was used as a substrate (Fig. 2, *C*, *lane 5*, and *D*). These experiments imply that Thr-716 on IQGAP2 is a preferred substrate site for PKA.

To verify this result we monitored the phosphorylation status of IQGAP2 in cells. V5-IQGAP2 proteins were expressed in COS cells. Intracellular cAMP was elevated upon application of the adenylyl cyclase activator forskolin (20 μM) and the phosphodiesterase inhibitor 3-isobutyl-1-methylxanthine (75 μM) for 10 min. IQGAP2 immune complexes were extracted from cell lysates and probed with a phospho-PKA substrates antibody that recognizes phosphorylated RRX*S*/T motifs (Fig. 2, *E*

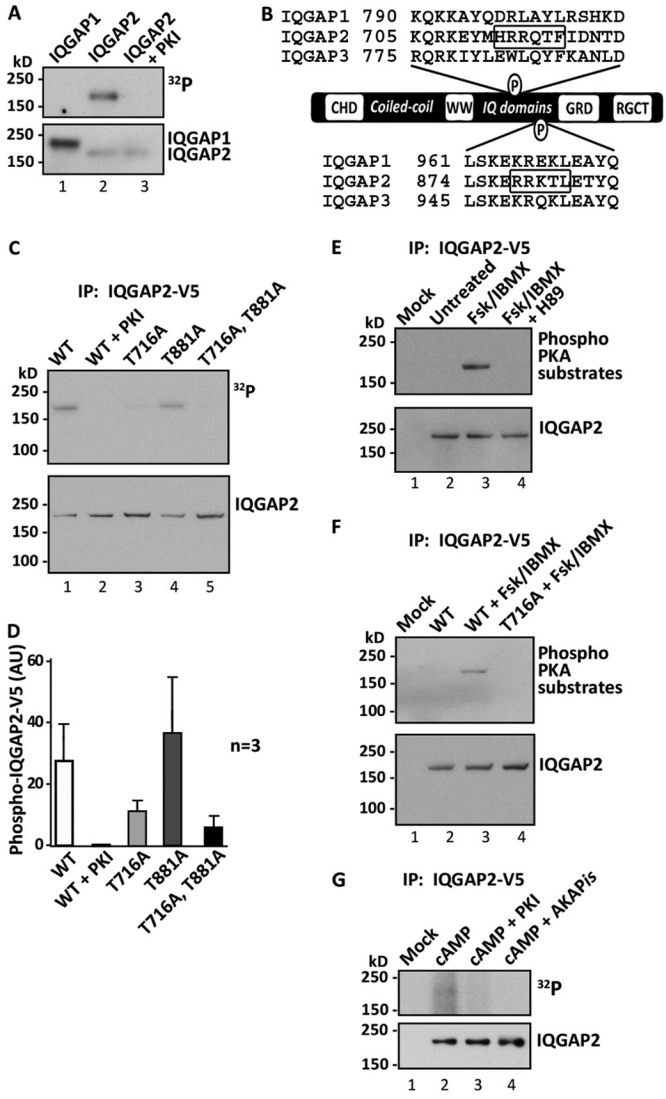

FIGURE 2. **IQGAP2 is a PKA substrate.** *A*, recombinant IQGAP1 and IQGAP2 expressed in HEK 293 cells were immunoprecipitated. Immune complexes were incubated with [^{32}P]ATP and purified PKA catalytic subunit. *Top*, autoradiograph detected phosphate ^{32}P incorporation into IQGAP1 (*lane 1*) and IQGAP2 (*lanes 2* and *3*). The PKI(5–24) peptide inhibitor was incubated with sample shown in *lane 3*. *Bottom*, IQGAP loading controls are shown. *B*, schematic diagram depicts the alignment of IQGAP proteins. Potential PKA phosphorylation sites (*boxed areas*) are identified on human IQGAP2 by Scansite motif scanner (60). *C*, V5-tagged IQGAP2 proteins were purified using an antibody toward the V5 tag. *In vitro* phosphorylation reactions were performed with [^{32}P]ATP and purified PKA catalytic subunit. *Top panel*, autoradiograph depicts ^{32}P incorporation into wild-type IQGAP2 (*lane 1*), wild-type IQGAP2 plus PKI(5–24) (*lane 2*), IQGAP2 T716A mutant (*lane 3*), IQGAP2 T881A mutant (*lane 4*), and IQGAP2 T716A/T881A double mutant (*lane 5*). *Bottom panel*, IQGAP2 loading controls are shown. *D*, densitometry analysis of amalgamated data from three experiments, mean ± S.E., are presented. *E* and *F*, PKA phosphorylated IQGAP *in situ*. *E*, *top panel*, immunoblotting detection used a phospho-PKA substrate site antibody of mock (*lane 1*), untreated IQGAP2 (*lane 2*), IQGAP2 isolated from COS cells exposed to elevated cAMP (*lane 3*), and IQGAP2 isolated from COS cells exposed to elevated cAMP in the presence of the PKA inhibitor H-89 (*lane 4*). *Bottom panel*, IQGAP2 loading controls are shown. *F*, *top panel*, immunoblotting detection used the phospho-PKA substrate site antibody of mock (*lane 1*), untreated IQGAP2 (*lane 2*), IQGAP2 isolated from COS cells exposed to elevated cAMP (*lane 3*), and a IQGAP2 T716A mutant (*lane 4*). *Bottom panel*, IQGAP2 loading controls are shown. *G*, *top panel*, autoradiograph depicts ^{32}P incorporation into V5-IQGAP2 purified from HEK 293 cell lysates mock control (*lane 1*), IQGAP2 plus cAMP (*lane 2*), IQGAP2 plus cAMP and PKI(5–24) (*lane 3*) and IQGAP2 plus cAMP and the anchoring inhibitor peptide AKAP-*is* (*lane 4*). Immunoblot controls showing the levels of IQGAP2 (*upper middle*) and AKAP220 (*lower middle*) present in IQGAP2 immune complexes and AKAP220 loading controls (*bottom*).

and *F*). Activation of endogenous PKA enhanced phosphorylation of wild-type IQGAP2 (Fig. 2*E*, *lane 3*). Pretreatment with the pharmacological inhibitor H-89 (10 μM, 20 min) blocked phosphorylation (Fig. 2*E*, *lane 4*). Additional experiments confirmed that the IQGAP2 T716A mutant could not be phosphorylated in cAMP-stimulated COS cells (Fig. 2*F*, *lane 4*). The data in Fig. 2 suggest that Thr-716 on IQGAP2 is phosphorylated by PKA inside cells.

The next step was to discern whether AKAP220-associated PKA catalyzed this phosphorylation event. V5-IQGAP2-AKAP220 complexes isolated from HEK 293 cell lysates were treated with cAMP (100 μM) and [^{32}P]ATP to activate the anchored PKA. The phosphorylation state of IQGAP was assessed by autoradiography to evaluate the contribution of the anchored kinase (Fig. 2*G*). Phosphorylation of IQGAP2 was stimulated upon exposure to cAMP (Fig. 2*G*, *top panel*, *lane 2*). Importantly, this effect was blocked in the presence of PKI(5–24) or upon treatment (5 μM) with the anchoring inhibitor peptide (38) AKAP-*is* (Fig. 2*G*, *top panel*, *lanes 3* and *4*). Immunoblots confirmed that equal levels of IQGAP2 and AKAP220 were present in each sample and that equal levels of the anchoring protein were present in the loading controls (Fig. 2*G*, *bottom panels*). These experiments suggest that the AKAP220-anchored pool of PKA phosphorylates IQGAP2.

Phosphorylation of IQGAP2 Augments Binding to the Small GTPase Rac—We reasoned that PKA phosphorylation of Thr-716 on IQGAP2 would have a functional consequence. This could either be to modulate IQGAP2 binding to AKAP220 or to enhance association with other binding partners. The first postulate was discarded when binding experiments suggested that modification of Thr-716 on IQGAP2 had no apparent effect on the interaction with AKAP220 (data not shown).

In keeping with our second postulate, the small GTPases have been shown to interact with IQGAP to drive actin-remodeling events at the periphery of cells (25, 39–41). Intracellular calcium contributes to this protein-protein interaction (29, 32), but there was reason to suspect that PKA phosphorylation could further augment the formation of this subcomplex. Therefore, we investigated whether PKA phosphorylation of Thr-716 on IQGAP2 might influence the recruitment of Rac. Cells expressing V5-IQGAP2 or the T716A mutant were treated with forskolin (20 μM) and 3-isobutyl-1-methylxanthine (75 μM). IQGAP2 immune complexes were probed for co-purification of Rac by immunoblotting. These experiments revealed that elevation of intracellular cAMP further enhanced Rac binding by 3-fold over nonstimulated controls (Fig. 3, *A*, *top panel*, *lane 3*, and *B*). Importantly, Rac binding was not detected in cells expressing the nonphosphorylatable IQGAP2 T716A mutant (Fig. 3*A*, *top panel*, *lane 4*). Control immunoblots confirmed that equivalent levels of Rac and IQGAP2 were used in each sample (Fig. 3*A*, *middle* and *bottom panels*). This allowed us to conclude that cAMP-responsive phosphorylation of Thr-716 on IQGAP2 augments interaction with Rac. Additional support for this concept was provided by evidence that Rac binding to the IQGAP2 T716D phosphomimetic mutant was enhanced 4.5-fold ($n = 4$) independently of cAMP (Fig. 3, *C*, *top panel*, *lane 4*, and *D*). Taken together, these results suggest that

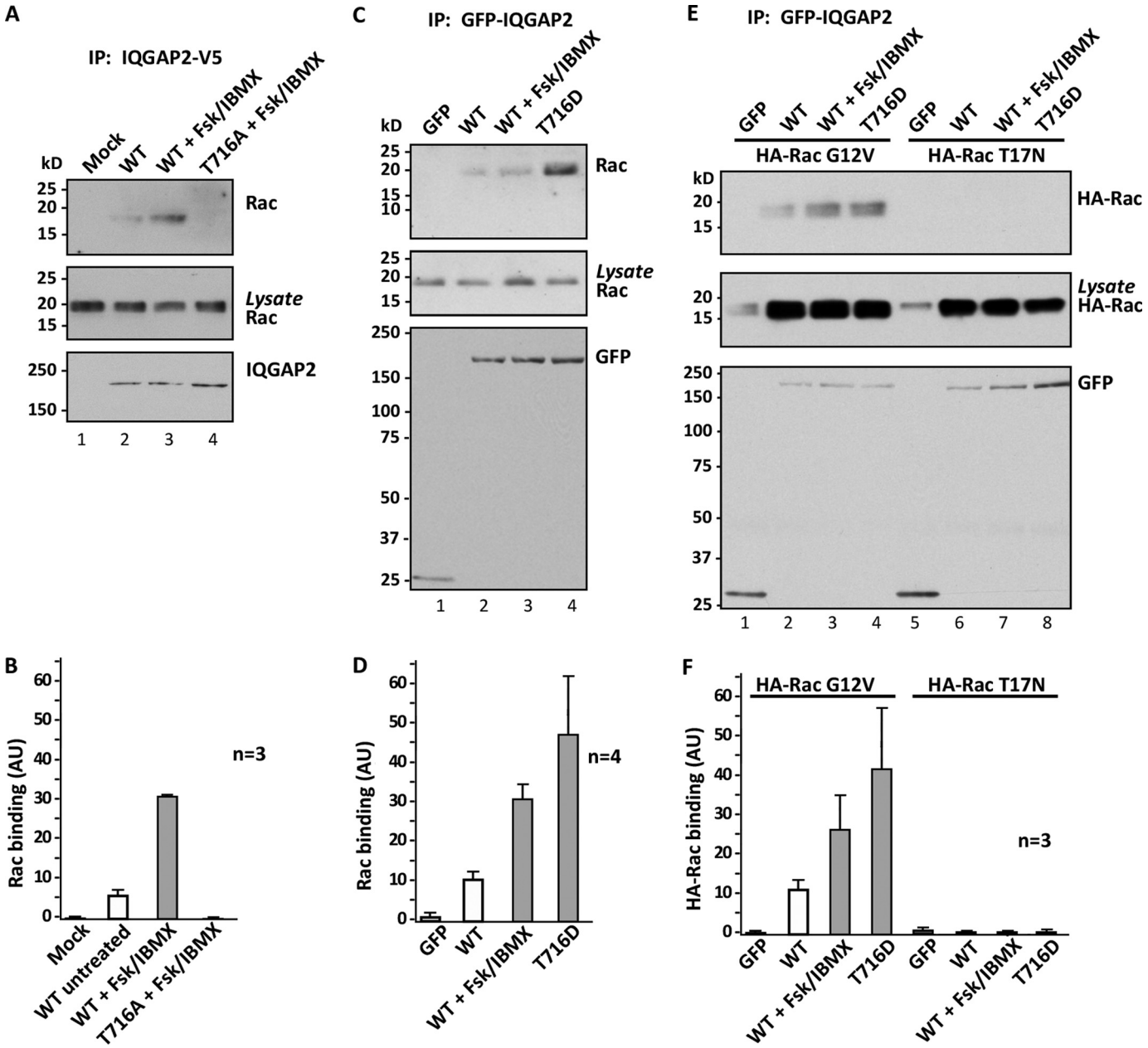

FIGURE 3. **Phosphorylation of IQGAP2 enhances binding to the Rac GTPase.** *A* and *B*, immunoblotting detects Rac co-immunoprecipitation with IQGAP2 from COS cells. *A*, *top panel*, experiments were performed with mock (*lane 1*), wild-type IQGAP2 isolated from control cells (*lane 2*), wild-type IQGAP2 isolated from cAMP-stimulated cells (*lane 3*), and IQGAP2 T716A mutant isolated from cAMP-stimulated cells (*lane 4*). Loading controls for Rac (*middle*) and IQGAP2 (*bottom*) are presented. *B*, densitometry analysis of amalgamated data from three experiments, mean ± S.E., is shown. *C* and *D*, Rac preferentially binds to the IQGAP2 T716D mutant. *C*, *top panel*, Rac co-immunoprecipitation with GFP-IQGAP2 was detected by immunoblot from GFP alone (*lane 1*), wild-type IQGAP2 isolated from control cells (*lane 2*), wild-type IQGAP2 isolated from cAMP-stimulated cells (*lane 3*), and the IQGAP2 T716D mutant (*lane 4*). Loading controls for Rac (*middle*) and IQGAP2 (*bottom*) are presented. *D*, densitometry analysis of amalgamated data from four experiments, mean ± S.E., is shown. *E*, *top panels*, experiments were repeated using the HA-tagged G12V constitutively active Rac mutant (*lanes 1–4*) or HA-tagged T17N dominant-interfering Rac mutant (*lanes 5–8*). Loading controls for HA-Rac mutants (*middle*) and GFP-IQGAP2 (*bottom*) are presented. *F*, densitometry analysis of amalgamated data from three experiments, mean ± S.E., is shown.

the association of Rac with the cytoskeletal scaffolding protein is regulated by phosphorylation of Thr-716 on IQGAP2.

IQGAPs preferentially bind to the active GTP-bound form of the small GTPases (25, 42). Accordingly, we were able to show that constitutively active Rac (HA-Rac G12V) preferentially bound to IQGAP2 (Fig. 3, *E*, *top panel*, *lanes 2–4*, and *F*), whereas the inactive Rac T17N form was refractory to this protein-protein interaction (Fig. 3, *E*, *top panel*, *lanes 6–8*, and *F*). It is worth noting that IQGAP may have the capacity to stabilize Rac and Cdc42 because we consistently observed increased levels of these proteins when they were co-expressed with GFP-tagged IQGAP2 (Fig. 3*E*, *middle panel*). Additional experiments indicate that formation of an IQGAP2-Rac G12V subcomplex is strengthened upon cAMP stimulation or with the IQGAP2 T716D phosphomimetic mutant (Fig. 3, *E*, *top panel*, *lanes 3* and *4*, and *F*).

The data in Fig. 3 argue that PKA phosphorylation of IQGAP2 on Thr-716 enhances association with the active form

of the small GTPase Rac. This is a unique property of IQGAP2, as this PKA site is not present in other IQGAP family members (Fig. 2*B*). Moreover, if Thr-716 phosphorylation occurs within the context of the AKAP220-IQGAP2 complex, it provides a means to help retain active Rac near the cell cortex. Interestingly, IQGAP also binds to Cdc42, a related GTPase that regulates different aspects of actin reorganization. Data presented as supplemental materials suggest that IQGAP2/Cdc42 interactions occur in a PKA-independent manner (supplemental Fig. S3). One interpretation of this finding is that Rac and Cdc42 use distinct surfaces to bind IQGAP2 and their binding may be regulated by different second messenger signals. This latter postulate is consistent with evidence that PKC phosphorylation on Ser 1443 of the IQGAP1 isoform favors association with nucleotide-depleted and inactive Cdc42 (43). An equivalent site is conserved in IQGAP2. Thus, phosphorylation of IQGAPs by PKA or PKCs may serve as a mechanism to modulate Rac and Cdc42 action differentially at the cell cortex. This sheds further light on the unique and enigmatic role of IQGAPs as accessory proteins for Rac and Cdc42 that function in a manner that is distinct from conventional GTPase-activating proteins or guanine nucleotide exchange factors (44).

Local Modulation of IQGAP and Rac Affects Actin Remodeling—IQGAPs and Rac act synergistically to drive actin cytoskeletal remodeling (32, 40). Therefore, we wondered whether AKAP220 might localize both proteins at sites of actin remodeling. Immunofluorescence detection revealed staining patterns for endogenous IQGAP2 (Fig. 4, *A* and *C*) and AKAP220 (Fig. 4, *D* and *F*) that overlap with cortical actin in HEK 293 cells (Fig. 4, *B* and *E*). Antibody compatibility issues prevented double labeling of AKAP220 with endogenous IQGAP2. However, staining patterns for V5-IQGAP2 and the anchoring protein overlap at cortical regions of HEK 293 cells (supplemental Fig. S4). Enrichment of AKAP220 at this location is consistent with the notion that binding partners PKA, IQGAP2, and Rac are well positioned to relay signals to the cortical actin cytoskeleton. Two approaches tested this hypothesis.

First we determined whether gene silencing of AKAP220 impacted remodeling of the cortical actin cytoskeleton. As a prelude to these studies, siRNA-mediated knockdown of the anchoring protein in cell lysates was confirmed (Fig. 4*G*, *top panel*, *lanes 2* and *3*). Immunoblot detection of actin was used as a loading control (Fig. 4*G*, *bottom panel*). Depletion of the anchoring protein from cortical regions was established by immunofluorescence microscopy (Fig. 4*K*). Knockdown of AKAP220 coincided with a reduction in actin-rich membrane ruffles (Fig. 4, *K–M*). Because rescue by overexpression of AKAP220 is toxic to cells, these data were duplicated with an independent siRNA that targets the anchoring protein (supplemental Fig. S5).

Control experiments confirmed that the location of AKAP220 and organization of the cortical actin cytoskeleton were unaffected in cells treated with a scrambled siRNA (Fig. 4, *H–J*). These results infer that AKAP220 contributes in some way to maintenance of the cortical actin cytoskeleton.

Second, GFP-IQGAP2 phosphorylation site mutants were expressed in HEK 293 cells to evaluate their impact on membrane ruffles. Paraformaldehyde fixation was used to preserve the structure of the actin cytoskeleton, and regions of membrane ruffling were detected with fluorescently conjugated phalloidin. Ruffles were identified through their unique morphology and quantified to calculate a ruffling index (ri). Cells without ruffles were scored as 0 whereas cells with 100% ruffling of their surface were given an arbitrary score of 3. This strategy has been described previously (28). Preliminary experiments established that expression of GFP had no discernable effect on the number or distribution of membrane ruffles (Fig. 5, *A–C* and *M*; GFP ri = 1.0 ± 0.01 (S.E.), $n = 59$). Overexpression of IQGAP2 modestly increased the numbers of membrane ruffles (Fig. 5, *D–F* and *M*, IQGAP2 ri = 1.42 ± 0.06, $n = 63$). However, expression of an IQGAP2 T716D phosphomimetic mutant increased numbers of membrane ruffles (Fig. 5, *G–I* and *M*, IQGAP2 T716D ri = 1.93 ± 0.1, $n = 49$). Expression of the nonphosphorylatable IQGAP2 T716A mutant had no effect (Fig. 5, *J–L* and *M*, IQGAP2 T716A ri = 1.0 ± 0.03, $n = 18$). Related experiments confirmed that disruption of PKA anchoring using a cell-soluble version of the Ht-31 disruptor peptide (45), or inhibiting PKA activity with H-89 had similar effects on F-actin (supplemental Fig. S6). The data in Figs. 4 and 5 argue that modification of Thr-716 on IQGAP2, which affects association with active Rac, drives changes in the actin cytoskeleton. Because these effects are suppressed upon gene silencing of AKAP220 we propose that the anchoring protein serves as an adaptor to bring enzyme to substrate.

Howe and Juliano discovered the link between PKA and Rho family GTPases (46). A role for AKAPs was subsequently defined by showing that peptide mediated disruption of PKA anchoring attenuated cAMP-responsive remodeling of the actin cytoskeleton (47). More recently, the extent to which individual AKAP complexes interface with Rho, Rac, and Cdc42 to promote different patterns of actin reorganization has come into clearer focus. For example, AKAP-Lbc contributes to stress fiber formation and cell movement by virtue of its guanine nucleotide exchange activity toward RhoA (48–50). PKA phosphorylation of Ser-1565 on AKAP-Lbc negatively regulates this process by initiating the phospho-dependent binding of 14-3-3 and blocking access to Rho (26, 51). A variation on this theme involves anchored PKA regulation of a related Rho exchange factor called Lfc (**L**bc's **f**irst **c**ousin). This proceeds through the Lfc-binding protein AKAP121. This slightly more elaborate configuration allows anchored PKA to favor the recruitment of 14-3-3 and thereby suppress the Lfc intrinsic Rho guanine nucleotide exchange activity (52). In a different cellular context, WAVE-1 organizes Rac-dependent mobilization of the Arp2/3 complex to promote actin cross-linking in neurons (53–55). Ablation of the WAVE-1 gene in the hippocampus impairs the formation of actin-rich dendrites and hampers the development of neuronal networks. As a result, WAVE-1-null mice show evidence of reduced excitatory synaptic transmission and display behavioral deficits in contextual learning and memory (56). Thus, AKAPs utilize a variety of mechanisms to manage Rho family GTPases as they shape the actin cytoskeleton.

In conclusion, we have shown that AKAP220 organizes an ensemble of binding partners that regulate actin-remodeling events. The key component is IQGAP2, a versatile scaffolding protein that has the capacity to engage both active Rac and

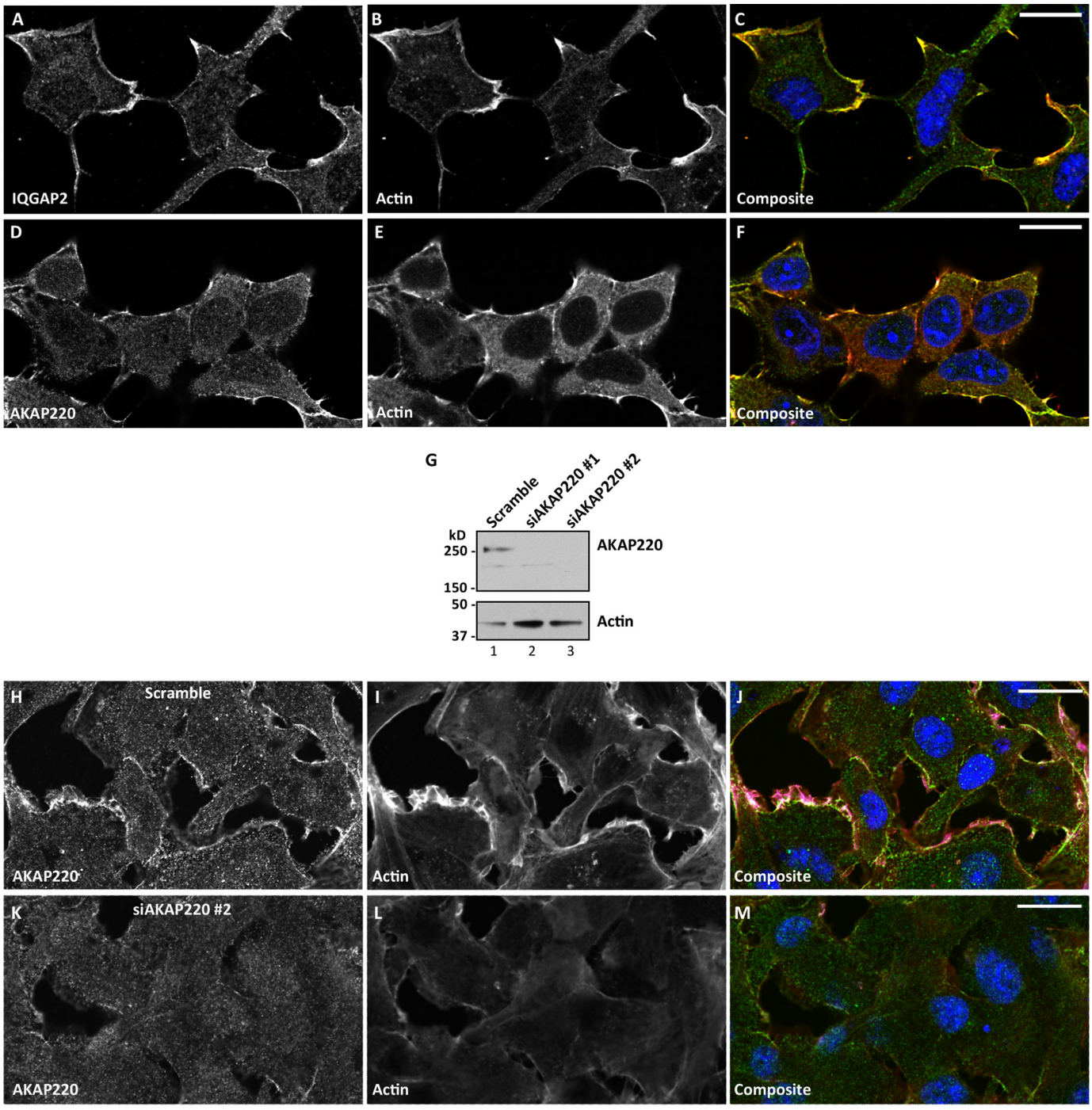

FIGURE 4. **IQGAP2 and AKAP220 are located near actin.** *A–C*, confocal immunofluorescence analysis of IQGAP2 (*A*, *green*) and actin (*B*, *red*) in HEK 293 cells. Nuclei were stained with DRAQ5 as indicated in the composite image (*C*, *blue*). *D–F*, subcellular distribution of AKAP220 (*D*, *green*) and actin (*E*, *red*). *F*, composite image including DRAQ5 staining of nuclei (*blue*). *G*, *top panel*, immunoblot confirmation of siRNA knockdown of AKAP220 in HEK 293 cells. The effects of scrambled siRNA (*lane 1*) and two different siRNAs (*lanes 2* and *3*) are shown. *Bottom panel*, actin loading controls. *H–N*, staining patterns for AKAP220 (*H* and *L*, *green*) and actin (*I* and *M*, *red*) in cells treated with control (*H–J*) and siAKAP220 (*K–M*). Nuclei were stained with DRAQ5 as indicated in the composite images (*K* and *N*). All *scale bars* indicate 20 μm.

Cdc42. There are two phases to this process. Calcium favors IQGAP2 association with AKAP220 (supplemental Fig. S2), and PKA phosphorylation of Thr-716 on IQGAP2 is necessary to recruit active Rac (Figs. 2 and 3). This tallies with evidence presented in Fig. 4 showing that the AKAP220-IQGAP2 complex is positioned to respond to activated Rac and that siRNA-mediated knockdown of AKAP220 shuts down Rac-mediated membrane ruffling. The final, and perhaps most compelling evidence is provided in Fig. 5, where overexpression of the IQGAP2 T716D phosphomimetic mutant increased membrane ruffles, whereas introduction of a nonphosphorylatable IQGAP2 form had no effect.

If one considers our conclusions in a broader perspective, they define a biological role for AKAP220-anchored PKA. We propose that AKAP220 not only spatially restricts the action of this notoriously promiscuous basophilic kinase, but also creates an environment where cAMP signals can be rapidly and pre-

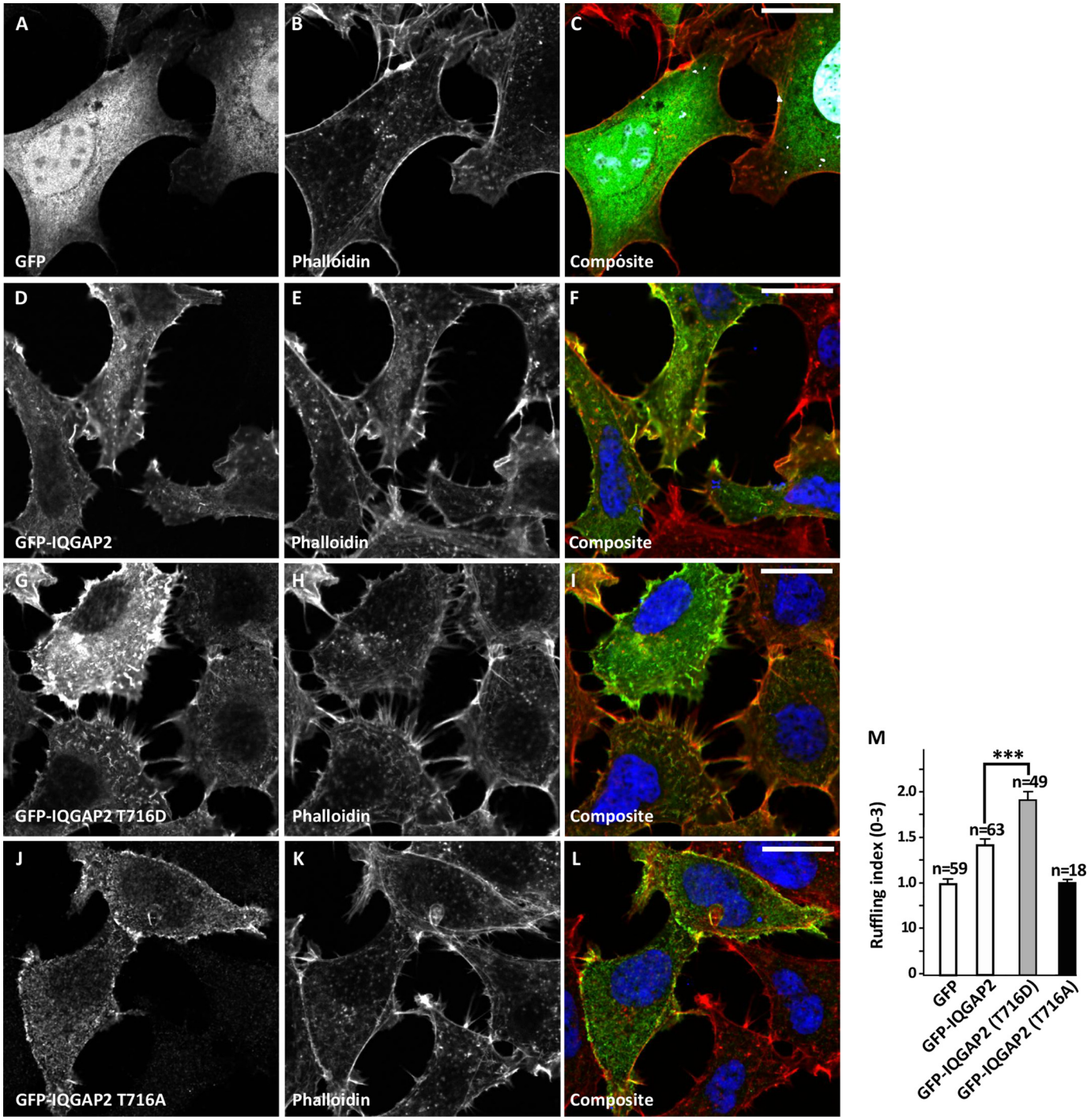

FIGURE 5. **IQGAP2 phosphorylation site mutants influence filamentous actin.** *A–C*, detection of GFP (*A*, *green*) and F-actin (*B*, *red*) in cultures of HEK 293 cells. F-actin was stained with fluorescently conjugated phalloidin. Nuclei were identified with DRAQ5 stain (*C*, *blue*). *D–F*, expression of GFP-tagged IQGAP2 in HEK 293 cells. *G–I*, expression of GFP-tagged IQGAP2 phosphomimetic mutant (T716D). *J–L*, nonphosphorylatable IQGAP2 mutant (T716A) expressed in HEK 293 cells. All *scale bars* indicate 20 μm. *M*, quantification of membrane ruffling. The number of cells analyzed in each condition is indicated above each *column*. Mean $\pm$ S.E. are shown, and *** indicates $p < 0.0001$.

cisely dispersed to the actin cytoskeleton. The strength and magnitude of these cAMP signals will depend on how much PKA is associated with AKAP220. Hence, defining the stoichiometry of this anchored-kinase complex is an important issue that will require additional investigation. These findings run counter to our earlier postulate that the AKAPs themselves would be prominent PKA substrates (57). Although this adage clearly holds true for AKAP-Lbc and Gravin (18, 58, 59) it seems that a majority of physiologically relevant PKA substrates are AKAP-binding partners, such as IQGAP2. This solidifies a current view that AKAPs are *bona fide* enhancers of cAMP-responsive signaling.

Acknowledgments—We thank the members of the Scott laboratory for critical evaluation of this manuscript and T. Pawson (Mt. Sinai Hospital Research Institute, Toronto) for mass spectrometry.

REFERENCES

1. Scott, J. D., and Pawson, T. (2009) *Science* **326,** 1220–1224
2. Bauman, A. L., and Scott, J. D. (2002) *Nat. Cell Biol.* **4,** E203–206
3. Wong, W., and Scott, J. D. (2004) *Nat. Rev. Mol. Cell. Biol.* **5,** 959–970
4. Pidoux, G., and Taskén, K. (2010) *J. Mol. Endocrinol.* **44,** 271–284
5. Scott, J. D., Stofko, R. E., McDonald, J. R., Comer, J. D., Vitalis, E. A., and Mangili, J. A. (1990) *J. Biol. Chem.* **265,** 21561–21566
6. Huang, L. J., Durick, K., Weiner, J. A., Chun, J., and Taylor, S. S. (1997) *J. Biol. Chem.* **272,** 8057–8064
7. Theurkauf, W. E., and Vallee, R. B. (1982) *J. Biol. Chem.* **257,** 3284–3290
8. Carr, D. W., and Scott, J. D. (1992) *Trends Biochem. Sci.* **17,** 246–249
9. Lohmann, S. M., DeCamilli, P., Einig, I., and Walter, U. (1984) *Proc. Natl. Acad. Sci. U.S.A.* **81,** 6723–6727
10. Dodge, K. L., Khouangsathiene, S., Kapiloff, M. S., Mouton, R., Hill, E. V., Houslay, M. D., Langeberg, L. K., and Scott, J. D. (2001) *EMBO J.* **20,** 1921–1930
11. Taskén, K. A., Collas, P., Kemmner, W. A., Witczak, O., Conti, M., and Taskén, K. (2001) *J. Biol. Chem.* **276,** 21999–22002
12. Dodge-Kafka, K. L., Soughayer, J., Pare, G. C., Carlisle Michel, J. J., Langeberg, L. K., Kapiloff, M. S., and Scott, J. D. (2005) *Nature* **437,** 574–578
13. Bauman, A. L., Soughayer, J., Nguyen, B. T., Willoughby, D., Carnegie, G. K., Wong, W., Hoshi, N., Langeberg, L. K., Cooper, D. M., Dessauer, C. W., and Scott, J. D. (2006) *Mol. Cell* **23,** 925–931
14. Dessauer, C. W. (2009) *Mol. Pharmacol.* **76,** 935–941
15. Kapiloff, M. S., Piggott, L. A., Sadana, R., Li, J., Heredia, L. A., Henson, E., Efendiev, R., and Dessauer, C. W. (2009) *J. Biol. Chem.* **284,** 23540–23546
16. Lester, L. B., Coghlan, V. M., Nauert, B., and Scott, J. D. (1996) *J. Biol. Chem.* **271,** 9460–9465
17. Schillace, R. V., and Scott, J. D. (1999) *Curr. Biol.* **9,** 321–324
18. Tanji, C., Yamamoto, H., Yorioka, N., Kohno, N., Kikuchi, K., and Kikuchi, A. (2002) *J. Biol. Chem.* **277,** 36955–36961
19. Noritake, J., Watanabe, T., Sato, K., Wang, S., and Kaibuchi, K. (2005) *J. Cell Sci.* **118,** 2085–2092
20. Johnson, M., Sharma, M., and Henderson, B. R. (2009) *Cell. Signal.* **21,** 1471–1478
21. White, C. D., Brown, M. D., and Sacks, D. B. (2009) *FEBS Lett.* **583,** 1817–1824
22. Fukata, M., Watanabe, T., Noritake, J., Nakagawa, M., Yamaga, M., Kuroda, S., Matsuura, Y., Iwamatsu, A., Perez, F., and Kaibuchi, K. (2002) *Cell* **109,** 873–885
23. Watanabe, T., Noritake, J., Kakeno, M., Matsui, T., Harada, T., Wang, S., Itoh, N., Sato, K., Matsuzawa, K., Iwamatsu, A., Galjart, N., and Kaibuchi, K. (2009) *J. Cell Sci.* **122,** 2969–2979
24. Mataraza, J. M., Briggs, M. W., Li, Z., Entwistle, A., Ridley, A. J., and Sacks, D. B. (2003) *J. Biol. Chem.* **278,** 41237–41245
25. Kuroda, S., Fukata, M., Kobayashi, K., Nakafuku, M., Nomura, N., Iwamatsu, A., and Kaibuchi, K. (1996) *J. Biol. Chem.* **271,** 23363–23367
26. Jin, J., Smith, F. D., Stark, C., Wells, C. D., Fawcett, J. P., Kulkarni, S., Metalnikov, P., O'Donnell, P., Taylor, P., Taylor, L., Zougman, A., Woodgett, J. R., Langeberg, L. K., Scott, J. D., and Pawson, T. (2004) *Curr. Biol.* **14,** 1436–1450
27. Corbin, J. D., and Reimann, E. M. (1974) *Methods Enzymol.* **38,** 287–290
28. Li, J., Brieher, W. M., Scimone, M. L., Kang, S. J., Zhu, H., Yin, H., von Andrian, U. H., Mitchison, T., and Yuan, J. (2007) *Nat. Cell Biol.* **9,** 276–286
29. Ho, Y. D., Joyal, J. L., Li, Z., and Sacks, D. B. (1999) *J. Biol. Chem.* **274,** 464–470
30. Li, Z., Kim, S. H., Higgins, J. M., Brenner, M. B., and Sacks, D. B. (1999) *J. Biol. Chem.* **274,** 37885–37892
31. Ren, J. G., Li, Z., and Sacks, D. B. (2008) *J. Biol. Chem.* **283,** 22972–22982
32. Briggs, M. W., and Sacks, D. B. (2003) *FEBS Lett.* **542,** 7–11
33. Carr, D. W., Stofko-Hahn, R. E., Fraser, I. D., Bishop, S. M., Acott, T. S., Brennan, R. G., and Scott, J. D. (1991) *J. Biol. Chem.* **266,** 14188–14192
34. Flockhart, D. A., Watterson, D. M., and Corbin, J. D. (1980) *J. Biol. Chem.* **255,** 4435–4440
35. First, E. A., Bubis, J., and Taylor, S. S. (1988) *J. Biol. Chem.* **263,** 5176–5182
36. Reinton, N., Collas, P., Haugen, T. B., Skålhegg, B. S., Hansson, V., Jahnsen, T., and Taskén, K. (2000) *Dev. Biol.* **223,** 194–204
37. Logue, J. S., and Scott, J. D. (2010) *FEBS J.* **277,** 4370–4375
38. Alto, N. M., Soderling, S. H., Hoshi, N., Langeberg, L. K., Fayos, R., Jennings, P. A., and Scott, J. D. (2003) *Proc. Natl. Acad. Sci. U.S.A.* **100,** 4445–4450
39. Wang, S., Watanabe, T., Noritake, J., Fukata, M., Yoshimura, T., Itoh, N., Harada, T., Nakagawa, M., Matsuura, Y., Arimura, N., and Kaibuchi, K. (2007) *J. Cell Sci.* **120,** 567–577
40. Mataraza, J. M., Li, Z., Jeong, H. W., Brown, M. D., and Sacks, D. B. (2007) *Cell. Signal.* **19,** 1857–1865
41. Brandt, D. T., and Grosse, R. (2007) *EMBO Rep.* **8,** 1019–1023
42. Kuroda, S., Fukata, M., Nakagawa, M., Fujii, K., Nakamura, T., Ookubo, T., Izawa, I., Nagase, T., Nomura, N., Tani, H., Shoji, I., Matsuura, Y., Yonehara, S., and Kaibuchi, K. (1998) *Science* **281,** 832–835
43. Grohmanova, K., Schlaepfer, D., Hess, D., Gutierrez, P., Beck, M., and Kroschewski, R. (2004) *J. Biol. Chem.* **279,** 48495–48504
44. Brown, M. D., and Sacks, D. B. (2006) *Trends Cell Biol.* **16,** 242–249
45. Carr, D. W., Hausken, Z. E., Fraser, I. D., Stofko-Hahn, R. E., and Scott, J. D. (1992) *J. Biol. Chem.* **267,** 13376–13382
46. Howe, A. K., and Juliano, R. L. (2000) *Nat. Cell Biol.* **2,** 593–600
47. Howe, A. K., Baldor, L. C., and Hogan, B. P. (2005) *Proc. Natl. Acad. Sci. U.S.A.* **102,** 14320–14325
48. Diviani, D., Soderling, J., and Scott, J. D. (2001) *J. Biol. Chem.* **276,** 44247–44257
49. Appert-Collin, A., Cotecchia, S., Nenniger-Tosato, M., Pedrazzini, T., and Diviani, D. (2007) *Proc. Natl. Acad. Sci. U.S.A.* **104,** 10140–10145
50. Paulucci-Holthauzen, A. A., Vergara, L. A., Bellot, L. J., Canton, D., Scott, J. D., and O'Connor, K. L. (2009) *J. Biol. Chem.* **284,** 5956–5967
51. Diviani, D., Abuin, L., Cotecchia, S., and Pansier, L. (2004) *EMBO J.* **23,** 2811–2820
52. Meiri, D., Greeve, M. A., Brunet, A., Finan, D., Wells, C. D., LaRose, J., and Rottapel, R. (2009) *Mol. Cell. Biol.* **29,** 5963–5973
53. Westphal, R. S., Soderling, S. H., Alto, N. M., Langeberg, L. K., and Scott, J. D. (2000) *EMBO J.* **19,** 4589–4600
54. Soderling, S. H., Binns, K. L., Wayman, G. A., Davee, S. M., Ong, S. H., Pawson, T., and Scott, J. D. (2002) *Nat. Cell Biol.* **4,** 970–975
55. Soderling, S. H., Guire, E. S., Kaech, S., White, J., Zhang, F., Schutz, K., Langeberg, L. K., Banker, G., Raber, J., and Scott, J. D. (2007) *J. Neurosci.* **27,** 355–365
56. Soderling, S. H., Langeberg, L. K., Soderling, J. A., Davee, S. M., Simerly, R., Raber, J., and Scott, J. D. (2003) *Proc. Natl. Acad. Sci. U.S.A.* **100,** 1723–1728
57. Scott, J. D., and McCartney, S. (1994) *Mol. Endocrinol.* **8,** 5–11
58. Carnegie, G. K., Smith, F. D., McConnachie, G., Langeberg, L. K., and Scott, J. D. (2004) *Mol. Cell* **15,** 889–899
59. Tao, J., Wang, H. Y., and Malbon, C. C. (2003) *EMBO J.* **22,** 6419–6429
60. Obenauer, J. C., Cantley, L. C., and Yaffe, M. B. (2003) *Nucleic Acids Res.* **31,** 3635–3641